JOURNAL OF MATERIALS SCIENCE **33** (1998) 5789–5794

Surface structure of the TiO_2 thin film photocatalyst

N. NEGISHI, K. TAKEUCHI, T. IBUSUKI
National Institute for Resources and Environment, Onogawa 16-3, Tsukuba, Ibaraki 305, Japan
E-mail: negishi@nire.go.jp

Control of the surface structure of titanium dioxide thin film photocatalysts was successfully carried out by a polymer-doped dip-coating process. The thin films prepared were either transparent or opaque, depending on the molecular weight of the polymer doped. All the thin film photocatalysts had anatase form with similar crystallinity. The surface of the transparent thin films looked plain consisting of uniformly aggregated nanometer-size TiO_2 particles, while the opaque thin films were formed of cubic crystalline TiO_2 at the micrometer level. Both the transparent and opaque films showed catalytic activity for the elimination of NO_x in air. The specific surface area and photocatalytic activity of the transparent thin film was almost the same as that of the opaque one. The activity of the thin films was almost equal to the commercial photocatalyst P25. Decrease in the film thickness led to a decrease of the elimination of NO in air by the thin films. The thin films were porous and the surface area was dependent on the film thickness. Adsorbed NO was photooxidized to NO_2 by the thin films, while the NO_2 formed was re-photooxidized to HNO_3 before the desorption of NO_2 from the film surface.

1. Introduction

Nitrogen oxides (NO_x, NO + NO_2) emitted from automobiles and combustion facilities are hazardous air pollutants [1]. High NO_x concentrations are often observed along highways, and removal techniques from the atmosphere are required. We have developed TiO_2-based photocatalysts that actively remove NO_x from ambient air [1, 2]. TiO_2 is a well-known photocatalyst and is a harmless white powder. The TiO_2 photocatalyst acts by UV irradiation at around the 360 nm region. We propose the use of the TiO_2 photocatalyst for the elimination of NO_x in open air and that the intensity of sunlight will be enough to activate the TiO_2. However, TiO_2 has one problem in the elimination of NO_x: The desorption of NO_2 from the TiO_2 photocatalyst surface is observed during the oxidative removal of NO, and such desorption must be suppressed because NO_2 is a regulated pollutant. An activated carbon-mixed TiO_2 photocatalyst was reported by Ibusuki *et al.* and Uchida *et al.* [1, 3]. Environmental pollutants and/or their intermediates (i.e., NO or NO_2) adsorb to the activated carbon, and they are completely oxidized to HNO_3 by the photocatalyst. However, developing activated photocatalytic material containing carbon is difficult. We have attempted to design an increase in the adsorption area of the thin film photocatalyst. By modifying the photocatalyst surface, the adsorption surface area for NO_2 must be obtained unless an adsorbent is used. It is known that highly photoactive thin film catalysts for the removal of acetaldehyde in the atmosphere are prepared from polymer-doped titanium alkoxide [4]. It is expected that the thin films have many micropores, and they act as a good catalyst for the elimination of NO_x, as well. In the present study, we prepared TiO_2 thin film photocatalysts by a dip-coating process using titanium alkoxide with organic or polymer compound additives [5]. The surface structure of the thin film has been elucidated, and their activity for the elimination of NO_x is discussed in terms of the surface structure.

2. Experimental procedure

A starting solution for the dip-coating process was prepared by mixing tetrapropyl orthotitanate (TPOT), ethanol, the organic/polymer additives, poly(ethylene) glycol (PEG) with an average molecular weight of 300 to 1000, and 2-(2-ethoxyethoxy)ethanol (EEE) (all the chemicals were obtained from Wako Chemical Industries, Ltd.). Approximately 700 ml of ethanol, 80 g of PEG, and 80 ml of EEE were mixed, and 80 ml of TPOT was continuously added to the mixed solution. Silica-coated glass plates ($10 \times 10 \times 0.1$ cm) were dip-coated with the solution under a relative humidity of 10%. The withdrawing speed of the substrates was 1.5 mm/s. The dip-coated glass plates were calcined at 450 °C for 1 h. This process was repeated to obtain a film of approximately 1 μm thickness. The thin film photocatalysts doped with PEG300, PEG600, and PEG1000 were designated as TiO_2-P300, TiO_2-P600, and TiO_2 -P1000, respectively, and a film without doping was designated as TiO_2-P0.

The film thickness was determined by the interference pattern of the transmittance spectra of the films.

The transmittance spectra were recorded with a Hitachi 330 spectrophotometer. The surface structure of the thin film was observed by atomic force microscopy (AFM, Shimadzu-9500). The crystal structure of the TiO_2 coatings was identified by X-ray diffraction (XRD, Mac Science; Cu$K\alpha$ radiation at 40 kV and 200 mA). Observation of the surface area was carried out by a Quantchrome AS-1. A flow type photoreactor was constructed to examine the photocatalytic activity of the films. The light intensity was about 0.38 mW/cm^2 ($\lambda = 365$ nm) at the photocatalyst surface. Dry air containing 1 ppm of NO was passed through the reactor at a rate of 1.5 l/min. The NO_x concentration was monitored with a chemiluminescent NO_x analyzer (Monitor Labs, Model 8440). The commercial photocatalyst powder, P25 (Degussa Co.) was used as the reference photocatalyst. The photocatalyst, 60 mg of P25, was spread onto the glass substrate over the same area of the thin film photocatalyst (10 × 10 cm). The weight of P25 (4.0 mg/cm^2) was almost the same as the film weight of TiO_2-P1000.

3. Results and discussion

3.1. Formation and characterization of thin film photocatalysts

The obtained thin films, TiO_2-P0, TiO_2-P300, and TiO_2-P600 were transparent, while TiO_2-P1000 was opaque. To obtain the 1 μm film thickness, 20 dippings were required, except for TiO_2-P0, which required about 50 dippings. Fig. 1 shows the transmittance spectra of the TiO_2 thin films. The absorption edge of the TiO_2 thin films apparently shifted as the film thickness increased (at around 340 nm with a 5-time dipping operation to around 360 nm with a 20-time operation). However, it is considered that this shift is not related to the quantum size effect [6] but is derived from the increase in the film thickness. The transparency of these films did not lessen with the increasing of dipping times, and the transmittance of these films in the visible region was around 80% except for TiO_2-P1000. As shown in Fig. 1, the wave pattern is attributed to the light interference. The number of interference peaks increased with the dipping times. It can be considered that the wavelengths at maximum or minimum light interference wave are correlated to the thickness, t, and the refractive index, n, of the film by the following equation [7].

$$n = \lambda_1\lambda_2/\{2t(\lambda_2 - \lambda_1)\} \quad (1)$$

where λ_1 and λ_2 indicate the wavelength of the adjacent pairs of the minima and maxima. We calculated the film thickness from the transmittance spectra using the assumed constant refractive index $n = 2.1$ [8]. Film thickness of TiO_2-P1000 could be calculated because light was penetrated despite the opaque film.

Fig. 2 shows the XRD profiles of the TiO_2 thin films, which show that an anatase was formed without any contamination of the other phase of TiO_2 [9, 10]. The crystallinity of each thin film was almost the same. We also observed the XRD pattern of the SiO_2 crystals ($d = 6.3$, 5.3, and 4.7). The peak intensity of the SiO_2 crystals is related to the size of the polymer doped into the TiO_2 thin films, and this intensity decreased with the increase in the doped polymer size except for TiO_2-P1000. This result indicates the film density. The thickness of each film is around 1 μm while the weight of thin film increased in the order of TiO_2-P0, TiO_2-P300, and TiO_2-P600. It is considered that the silica layer of the substrate could be observed through the TiO_2 layer by XRD investigations.

Fig. 3 shows the AFM images of the TiO_2-P600 surface. The surface structure of the other transparent

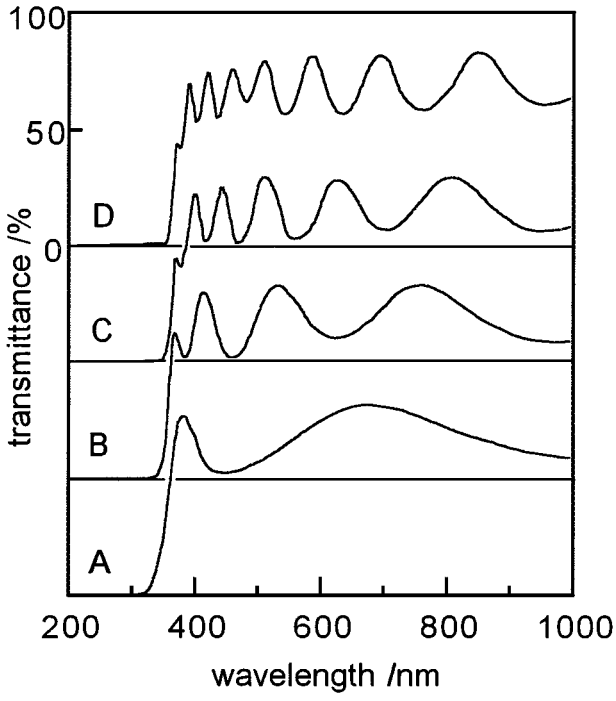

Figure 1 Transmittance spectra of TiO_2-P600 with increase in dipping time: (A) 5 times; (B) 10 times; (C) 15 times; and (D) 20 times.

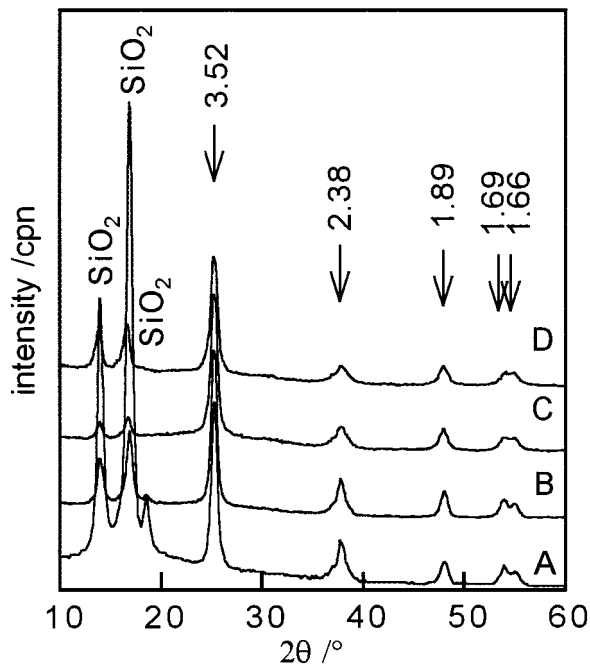

Figure 2 XRD pattern of thin films: (A) TiO_2-P0; (B) TiO_2-P300; (C) TiO_2-P600; and (D) TiO_2-P1000.

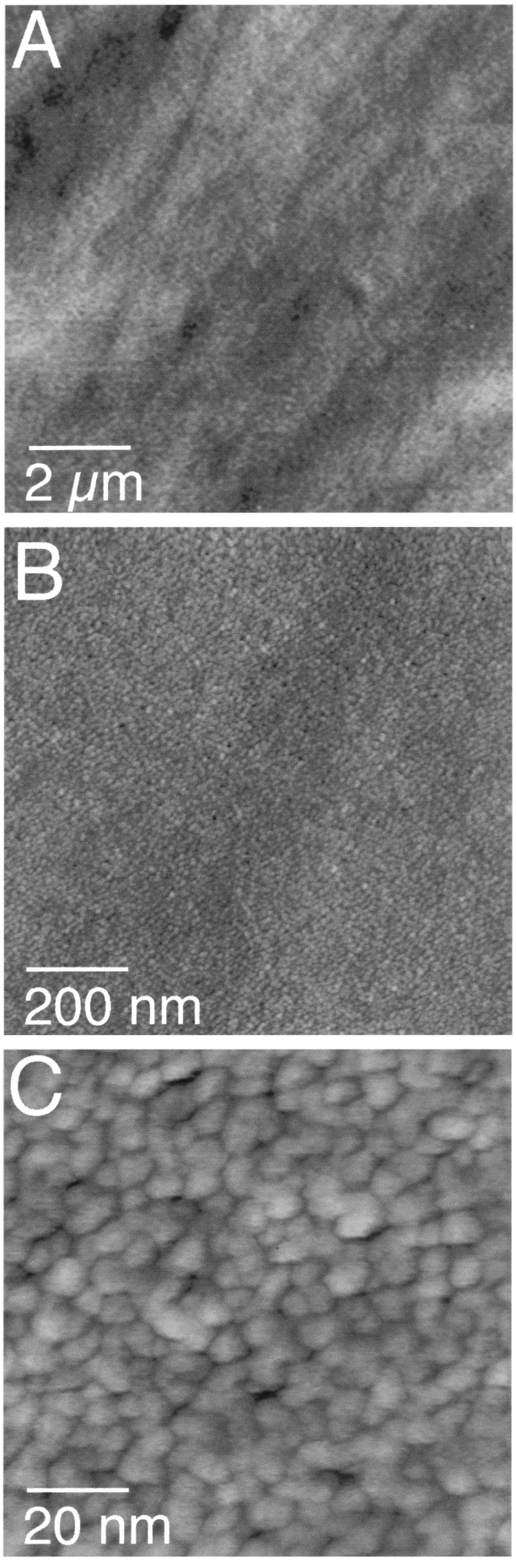

Figure 3 AFM images of the TiO_2-P600 surface: (A) 10 × 10 μm; (B) 1 × 1 μm; (C) 0.1 × 0.1 μm.

samples (TiO_2-P300 and TiO_2-P0) was almost the same as TiO_2-P600. As shown in Fig. 3a, b, the surfaces of the transparent films are very flat at the micrometer regions. The transparent film was constructed with smoothly aggregated nano-sized TiO_2 particles, as shown in Fig. 3c, and the particle size was around 5 nm in diameter. These particles consist of a single crystal of TiO_2. From the half-width of the XRD pattern of the thin films, the crystal size of TiO_2 was determined to be around 4 nm. This result is in good agreement with the AFM image of the thin films.

Fig. 4 shows the AFM image of the TiO_2-P1000 surface. As shown in Fig. 4a, TiO_2-P1000 reveals a different structure than that of TiO_2-P600. The surface of TiO_2-P1000 was made from aggregated cubic TiO_2 crystals of approximately 0.5 μm. The XRD pattern shows that the crystal size of TiO_2-P1000 was around 4 nm, as was the size of the other thin films shown in Fig. 2; it is considered that this crystal has a polycrystalline structure. However, we could not observe any boundary on the cubic TiO_2 crystal, as shown in Fig. 4c.

This striking difference in the surface structure between transparent films such as TiO_2-P600 and the opaque film such as TiO_2-P1000 may be explained in terms of the hydrolysis of TPOT and polymer. It is known that metal alkoxide is coordinated with diols such as 2-methyl-2, 4-pentanediol in mixed solution, and this coordination controls the hydrolysis rate of metal alkoxide [11]. As will be discussed, the larger size of polyethyleneglycol weakens the interaction between ligand and alkoxide, or the large size of the polymer prevents the coordination between TPOT and EEE. As a result, the hydrolysis of metal alkoxide is accelerated by the water in the atmosphere (i.e., humidity) and may be caused by the separation between the inorganic phase and the organic phase [11, 12]. For the PEG1000-doped TPOT solution system, doped polymer is separated from TiO_2 in the withdrawing process. The separated TiO_2 is localized and forms an aggregation, while the aggregated TiO_2 changes to a polycrystalline phase on the substrate by the calcination process. Many TiO_2 polycrystals are formed by repeating this withdrawing process, and the opaque film was obtained. This competitive reaction between metal alkoxide hydrolysis and phase separation may be explained by spinodal phase separation [13].

Fig. 5 shows the AFM image of the TiO_2-P1000 surface after one dipping. The TiO_2 polycrystals form and disperse on the substrate as an island with just one dipping. The microparticles grew and accumulated heterogeneously with an increasing number of dippings. Finally, the TiO_2 large-particle-accumulated-structure was formed, as shown in Fig. 4a.

In the case of PEG600 and PEG300, the doped polymer and TiO_2 do not localize in the film because the hydrolysis rate of TPOT is not so fast, and the homogeneity of the polymer–TPOT mixture may be maintained in the withdrawing process. TiO_2 does not crystallize in a large size, because titanium alkoxide may be dispersed in the polymer matrix during calcination. As a result, very small particles and pores were formed

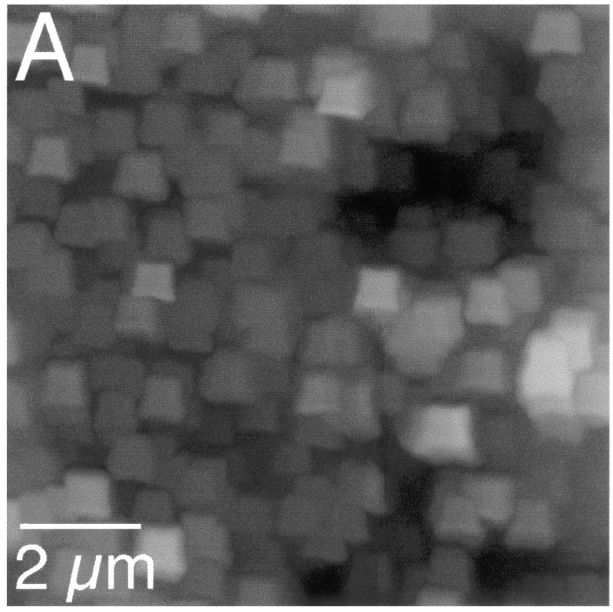

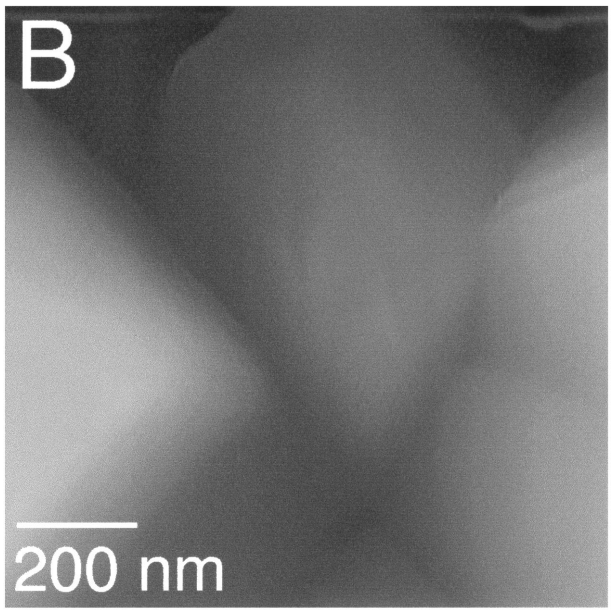

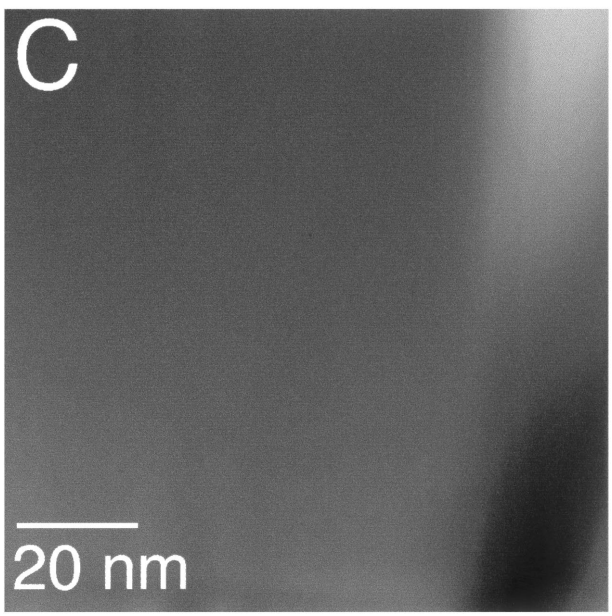

Figure 4 AFM images of the TiO_2-P1000 surface: (A) 10 × 10 μm; (B) 1 × 1 μm; and (C) 0.1 × 0.1 μm.

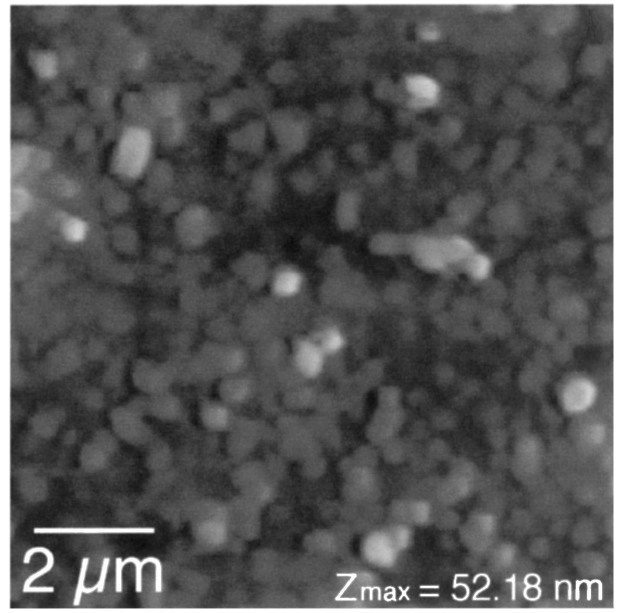

Figure 5 AFM images of the TiO_2-P1000 surface dipped one time (compare with Fig. 4a). (A) 10 × 10 μm.

after the calcination process with the evaporation of organic compounds, and transparent film was obtained.

Humidity is another important factor to control the transparency (i.e., control of the surface structure) of the films. Under a humid atmosphere (over 20% relative humidity), the PEG600-doped system produced an opaque film the same as TiO_2-P1000. These results show that a higher humidity decreases the interaction between TPOT and the polymer.

3.2. Photocatalytic ability of the thin film photocatalysts

Fig. 6 shows the time course of the changes in the NO and NO_2 concentration by the thin film photocatalyst with the differences in film thickness. The experimental system for the evaluation of the photocatalytic ability for deNO*x* was the same as used by Takeuchi [14]. The film thicknesses of the photocatalyst for the photooxidation of NO were 1, 0.5, and 0.25 μm. The photocatalytic ability of the thin films was drastically changed with the film thickness. As shown in Fig. 6a, the amount of NO removal by 1 μm of thin film was higher in the other thin films and P25. The photocatalytic ability of 1 μm of thin film was higher than P25 at the same weight (approximately 60 mg) and the illuminated area (100 cm^2) of the thin films. On the other hand, the amount of NO_2 formed by 1 μm of the thin film was lower than for the other thin films.

NO is converted to HNO_3 with photooxidation by way of NO_2.

$$NO + 1/2O_2 \xrightarrow[TiO_2]{h\nu} NO_2 \quad (2)$$

$$2NO_2 + 1/2O_2 + H_2O \xrightarrow[TiO_2]{h\nu} 2HNO_3 \quad (3)$$

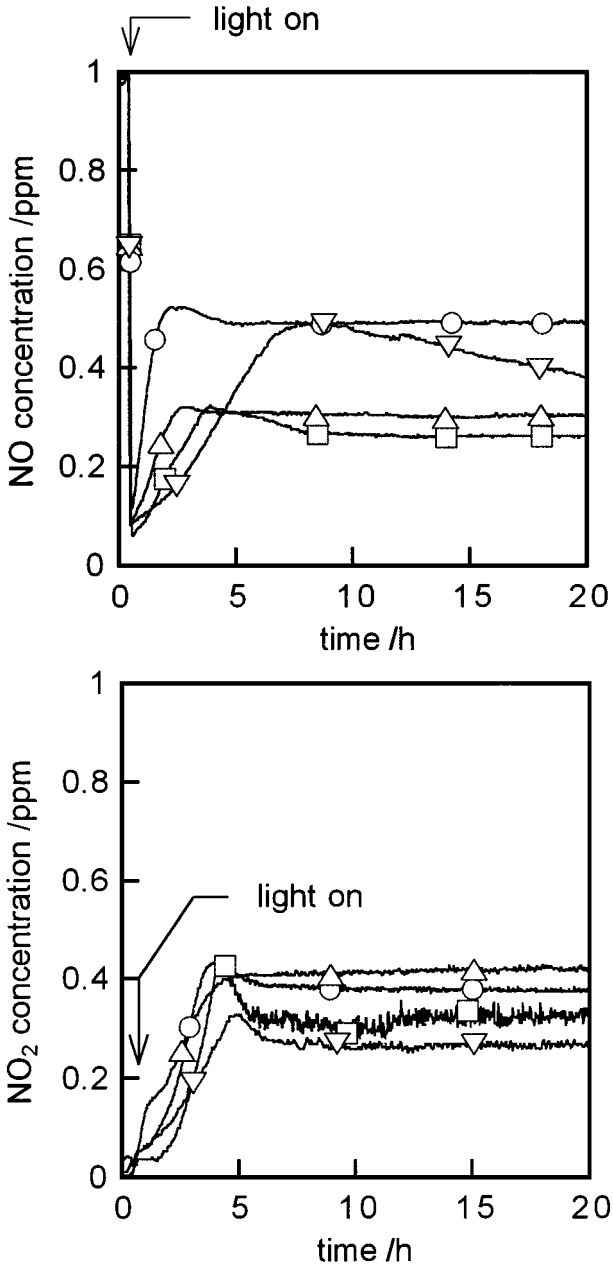

Figure 6 Time-course of the concentration of NO and NO_2 in the presence of TiO_2-P600 and P25 with different film thicknesses: (A) NO; (B) NO_2 (□: 1 μm thick; Δ: 0.5 μm thick; ○: 0.25 μm thick; and ∇: 60 mg of P25).

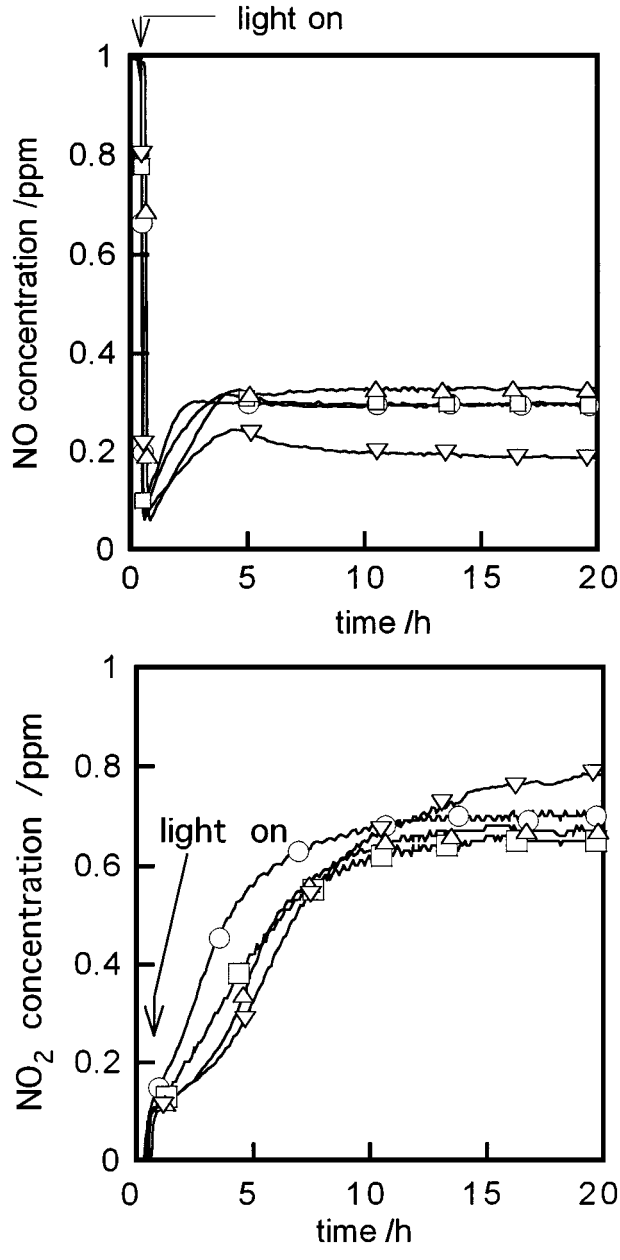

Figure 7 Time-course of the concentration of NO and NO_2 in the presence of the catalyst: (A) NO; (B) NO_2 (□: TiO_2-P0; Δ: TiO_2-P300; ○: TiO_2-P600; ∇: TiO_2-P1000).

The decrease in photocatalytic activity of the catalysts after photoirradiation was attributed to the coverage of the catalyst surface by the HNO_3 formed. Hydrogen formed HNO_3 from NO_2 on the TiO_2 thin films, as shown in Equation 3, because the carrier gas of NO did not include the humidity in our experimental system. It was considered that hydrogen was supplied from the surface hydroxyl groups and adsorbed water of TiO_2. It is easily expected that 1 μm of the film has a larger surface area than the other thin films. This large surface area leads to much adsorbed water, and adsorbed NO_2 can be easily photooxidized to HNO_3 before desorption. All of the adsorbed water is spent in the reaction for the formation of HNO_3 by the re-oxidation of NO_2, and the increase in HNO_3 is caused by saturation. However, the photocatalytic ability was decreased when the surface of the films was covered with excessive adsorption water under high humid conditions. In the case of the 1 μm thick film, after the saturation of the HNO_3 formation, the stoichiometric ratio between the removed NO and the NO_2 was attained after photoirradiation for 12 h. From these results, the most suitable film thickness is 1 μm.

Fig. 7 shows the time dependence of the elimination of NO and NO_2 by the photocatalysts. The average NO removal by TiO_2-P300, TiO_2-P600, and TiO_2-P1000 was 65, 70, and 81%, respectively, while that of TiO_2-P0 was about 71%. As shown in Fig. 7, the amount of NO_2 from the transparent film desorbed was almost same as the opaque one. The photocatalytic activity of the TiO_2 thin films were expected to change by the modification of the surface structure of the thin films. However, the amount of NO_2 desorbed from the thin film did not vary with the other thin films. The surface areas of each film was thus measured. The BET

surface area of TiO_2-P0, TiO_2-P300, TiO_2-P600, and TiO_2-P1000 was 112, 104, 118, and 141 m^2/g, respectively. These specific surface areas are twice those of P25 (approximately 50 m^2/g). This result indicates that the difference of specific surface area of these thin films is not so large, and the photocatalytic activity is almost the same. The reason why there was no significant difference in the surface area despite the large difference in the crystal size was considered as follows: The surface area of opaque film may be attributed to the complex structure at the micrometer scale region. On the other hand, the transparent thin films consist of many nanometer crystals, leading to the large surface area.

4. Conclusions

The control of the surface structure of the TiO_2 thin films can be carried out by doping the polymer into the titanium alkoxide solution. The crystal structure of the film photocatalyst has only an anatase. The surface structure of the thin films was markedly changed with the sort of polymer doped. These results show that the difference in the hydrolysis rate of the titanium alkoxide changes with the size of the polymer doped, depending on the interaction between the titanium alkoxide and polymer. Photocatalytic activity of the thin films depended on the film thickness. It is obvious that the thin film photocatalyst with a large surface area has a higher activity for the elimination of NO. On the other hand, we could not observe the differences in photocatalytic abilities of the thin films with different sizes of doped polymer. This result explains that the surface area of the thin films with difference sizes of doped polymer is almost the same.

References

1. T. IBUSUKI and K. TAKEUCHI, *J. Molec. Catal.* **88** (1994) 93.
2. K. TAKEUCHI, *Kagaku to Kogyo* **46** (1993) 61.
3. H. UCHIDA, S. ITOH and H. YONEYAMA, *Chem. Lett.* (1993) 1995.
4. N. NEGISHI, T. IYODA, H. HASHIMOTO and A. FUJISHIMA, *ibid.* (1995) 841; N. Negishi, K. Takeuchi, and T. Ibusuki, *Appl. Surf. Sci.*, **121/122** (1997) 417.
5. K. KATO, A. TSUZUKI, Y. TORII, H. TAODA, T. KATO and Y. BUTSUGAN, *J. Mater. Sci.* **30** (1995) 837; K. Kato, A. Tsuzuki, H. Taoda, Y. Torii, T. Kato, and Y. Butsugan, *ibid.* **29** (1994) 5911.
6. N. SERPONE, D. LAWLESS, and R. KHAIRUTDINOV, *J. Phys. Chem.* **99** (1995) 16646.
7. Y. TAKAHASHI and Y. MATSUOKA, *J. Mater. Sci.* **23** (1988) 2259.
8. T. NISHIDE and F. MIZUKAMI, *J. Ceram. Soc. Jpn.* **100** (1992) 1122.
9. M. TOBA, *Shokubai* **36** (1994) 319.
10. H. KOMINAMI, Y. TAKADA, H. YAMAGIWA and Y. KERA, *J. Mater. Sci. Lett.* **15** (1996) 197.
11. K. NAKANISHI and N. SOGA, *J. Non-Cryst. Solids* **139** (1992) 1; *Idem., ibid.* **142** (1992) 36.
12. K. D. JANDT, J. HEIER, F. S. BATES and E. J. KRAMER, *Langmuir* **12** (1996) 3716.
13. K. NAKANISHI and N. SOGA, *Bull. Chem. Soc. Jpn.* **70** (1997) 587.
14. K. TAKEUCHI, K. TOYOSE, S. KUTSUNA and T. IBUSUKI, *Shigen to Kankyo* **3** (1994) 103.

Received 4 December 1997
and accepted 17 July 1998